

# ChemComm

Chemical Communications

[www.rsc.org/chemcomm](http://www.rsc.org/chemcomm)

Volume 47 | Number 9 | 7 March 2011 | Pages 2457–2716



ISSN 1359-7345

RSC Publishing

**COMMUNICATION**

Ken Cham-Fai Leung *et al.*

Hierarchical core/shell  $\text{Fe}_3\text{O}_4@ \text{SiO}_2@ \gamma\text{-AlOOH}@ \text{Au}$  micro/nanoflowers for protein immobilization

Cite this: *Chem. Commun.*, 2011, **47**, 2514–2516

www.rsc.org/chemcomm

COMMUNICATION

## Hierarchical core/shell $\text{Fe}_3\text{O}_4@\text{SiO}_2@\gamma\text{-AlOOH}@Au$ micro/nanoflowers for protein immobilization†

Shouhu Xuan,<sup>ac</sup> Feng Wang,<sup>a</sup> Xinglong Gong,<sup>c</sup> Siu-Kai Kong,<sup>b</sup> Jimmy C. Yu<sup>a</sup> and Ken Cham-Fai Leung<sup>\*a</sup>

Received 6th December 2010, Accepted 12th January 2011

DOI: 10.1039/c0cc05390b

**A facile synthesis of monodispersed microparticles composed of superparamagnetic  $\text{Fe}_3\text{O}_4$  cores,  $\text{SiO}_2$  shell, hierarchical  $\gamma\text{-AlOOH}$  periphery with Au nanoparticles is reported. These particles are found to be useful for protein immobilization and bear resemblance to daisy flowers, and are hereafter termed “nanoflowers”.**

Hierarchical nanoarchitectures assembled from nanoscale units have recently stimulated tremendous interest because these superstructures might avoid aggregation and maintain high specific surface areas.<sup>1</sup> A large number of exotic nanostructures that exhibit novel physical, chemical, and biological properties have been fabricated and have demonstrated their potential as catalysts, sensor, separation and absorbent materials.<sup>2</sup> Self-organization of hierarchical nanoarchitectures with other meaningful components together to form core/shell nanostructures renders it possible to achieve materials with unique structures and functions.<sup>3</sup> A self-assembly process would lead to ordered aggregates formed in a spontaneous process.<sup>4</sup> However, it is somewhat of a challenge to construct hierarchical components directly based on any core structure. There are literature reports on the preparation of hierarchical nanostructures by using naked  $\text{SiO}_2$  or surface modified colloid particles as templates.<sup>4,5</sup> The sol–gel coating approach has been proven to be a facile and effective method for preparation of  $\text{SiO}_2$  coated composite nanoparticles.<sup>6</sup> Therefore, in principle, a straightforward strategy for the synthesis of composite material with a hierarchical nanostructure, and a  $\text{SiO}_2$  protected functional core, is yet to be developed.

Magnetic materials have gained much attention due to their unique separable features to selectively capture interesting

target objects from complex mixtures, for magnetic controllable drug delivery, and magnetic recycling nanocatalysts.<sup>7</sup> Several magnetic separation systems based on magnetic nanocomposites have been reported in an effort to achieve easy separation and manipulation of recombinant proteins.<sup>8</sup> However, there are only a few reports on the preparation of monodispersed superparamagnetic core/shell microparticles with hierarchical nanostructures, partly because of the difficulty in direct immobilization of hierarchical units onto the magnetic cores. In considering the high surface areas and any other new functionality of the hierarchical nanoarchitectures, it has been recognized that the incorporation of magnetic materials into the hierarchical nanoshells can provide new opportunities for improving their performance in practical applications.

The synthetic procedure for the monodispersed nanoflowers is illustrated in Fig. 1. By way of an example, the first step involves the uniform coating of a superparamagnetic  $\text{Fe}_3\text{O}_4$  microsphere (200 nm)<sup>6</sup> with a layer of  $\text{SiO}_2$  (25 nm) to produce spherical  $\text{Fe}_3\text{O}_4@\text{SiO}_2$  core/shell particles (Fig. S2a,b). The size of the  $\text{Fe}_3\text{O}_4$  sphere and the shell thickness of the  $\text{SiO}_2$  coating are controllable by using the solvothermal reaction and a sol–gel process.<sup>6</sup> The  $\text{SiO}_2$  coating not only protects the  $\text{Fe}_3\text{O}_4$  core but also modifies the surface

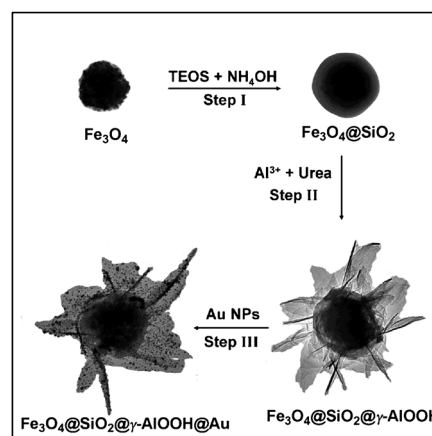


**Fig. 1** Graphical representation of the fabrication of monodispersed flower-like structure with superparamagnetic core and hierarchical shell.

<sup>a</sup> Center of Novel Functional Molecules and Institute of Molecular Functional Materials, Department of Chemistry, The Chinese University of Hong Kong, Shatin, NT, Hong Kong SAR, P. R. China. E-mail: cfleung@cuhk.edu.hk; Tel: (+852) 2609 6342

<sup>b</sup> School of Life Sciences, The Chinese University of Hong Kong, Shatin, NT, Hong Kong SAR, P. R. China

<sup>c</sup> CAS Key Laboratory of Mechanical Behavior and Design of Materials, Department of Modern Mechanics, The University of Science and Technology of China, Hefei, 230026, P. R. China

† Electronic supplementary information (ESI) available: Additional characterization data and experimental procedures. See DOI: 10.1039/c0cc05390b

properties, which is beneficial to the subsequent solvothermal formation of hierarchical  $\gamma$ -AlOOH nanosheets to give the nano/microflower structures. In the third step, the nanoflowers were modified by 3-aminopropyltriethoxysilane to functionalize the particles with amine functional groups and then protonated into ammonium groups. Negatively charged, citrate-protected Au nanoparticles (4 nm) were effectively assembled onto the positively charged nanoflower surface *via* electrostatic attraction.<sup>9</sup> The final product was then investigated for protein immobilization and separation.

The morphology of the particles was examined by using scanning electron microscopy (SEM) and transmission electron microscopy (TEM). Fig. 2a shows the SEM image of a typical sample that contains many uniform, flower-like architectures with a diameter of approximately 500 nm. The detailed morphology of the flower-like structures is shown in Fig. 2b and its inset, which reveal that the periphery of the structure is composed of many nanosheets with a thickness of 5–10 nm and 100–300 nm wide. As-prepared nanoflowers are monodispersed and can be well dispersed in the solution without large aggregation (Fig. 2a and c). The core/shell nanostructure is clearly revealed by the typical TEM image for a single nanoflower in Fig. 2d, from which it is apparent that the  $\text{Fe}_3\text{O}_4$  core is well encapsulated with a  $\text{SiO}_2$  coating. There are many nanosheets immobilized on the surface of the  $\text{SiO}_2$  shell. Fig. 2e–h reveal the high-resolution TEM images of the interface between  $\text{SiO}_2$  shell and hierarchical  $\gamma$ -AlOOH nanosheets, which clearly indicates their tight connection whereas the immobilized hierarchical  $\gamma$ -AlOOH nanosheet is a curving lamella with a thickness of *ca.* 4 nm.

The energy-dispersive X-ray (EDX) spectrum (using carbon-coated copper grid) of the nanoflower indicates the presence of Fe, Al, Si, and O, thereby proving the presence of  $\text{Fe}_3\text{O}_4$ ,  $\text{SiO}_2$ , and  $\gamma$ -AlOOH (Fig. 2i). The crystallographic structure and composition of the nanoflowers are examined by X-ray

powder diffraction (XRD) (Fig. S1), showing clearly the immobilization of  $\gamma$ -AlOOH onto the surface of the  $\text{Fe}_3\text{O}_4@/\text{SiO}_2$  core/shell particles. No other signals related to possible impurities such as  $\text{Al}_2\text{O}_3$  are detected in the products.

This unique multi-component nanostructure was fabricated by combining the versatile TEOS sol-gel process and interfacial deposition of  $\gamma$ -AlOOH. The  $\text{Fe}_3\text{O}_4@/\text{SiO}_2$  core/shell microspheres were dispersed in a water-ethanol mixture whereas  $\text{Al}^{3+}$  and urea were dissolved. During the hydrothermal process, aluminate anions would be formed under the high alkaline condition which is generated by the urea decomposition. At high temperature, the aluminate anions would be transformed into  $\text{Al}(\text{OH})_3$  colloids. The newly formed  $\text{Al}(\text{OH})_3$  colloids are reactive and unstable, and would be further dehydrated and converted into  $\gamma$ -AlOOH.<sup>10</sup> The Si–O bond of the  $\text{SiO}_2$  shell would be broken in the alkaline condition, and this leads to the consumption of hydroxide ions,<sup>11</sup> which could further promote the formation of  $\gamma$ -AlOOH.<sup>4b</sup>  $\gamma$ -AlOOH is a layered structure with octahedral array within the lamellae and that hydroxyl ions hold the integrity of lamellae together through hydrogen bonding interactions. Thus,  $\gamma$ -AlOOH nanosheet was generated only in basic conditions.<sup>4b,c</sup> When naked  $\text{Fe}_3\text{O}_4$  particle is used as the template, the complementary interactions between the  $\text{Fe}_3\text{O}_4$  and  $\gamma$ -AlOOH are somewhat weak, leading to a failure in the formation of flower-like nanostructures. Therefore, the  $\gamma$ -AlOOH nanosheet is preferentially generated around the  $\text{SiO}_2$  shell and deposited onto the periphery of the  $\text{Fe}_3\text{O}_4@/\text{SiO}_2$  core/shell microspheres.

By carefully examining the TEM image of the  $\text{Fe}_3\text{O}_4@/\text{SiO}_2@/\gamma$ -AlOOH nanoflower structures (Fig. S2c), a blank boundary is observed between the  $\text{Fe}_3\text{O}_4$  core and  $\text{SiO}_2$  shell, from which it is apparent that some void space existed. In comparison with the  $\text{Fe}_3\text{O}_4@/\text{SiO}_2$  precursor, the void space is generated during the hydrothermal process and is responsible for partial hydrolysis/etching of  $\text{SiO}_2$ . That is, the  $\text{SiO}_2$  shell was a reactive template for  $\gamma$ -AlOOH nanosheet formation. After the reaction was conducted for 36 h, many nanosheets existed on the surface of the  $\text{Fe}_3\text{O}_4@/\text{SiO}_2$  microspheres and only a few voids were present between the  $\text{Fe}_3\text{O}_4$  core and  $\text{SiO}_2$  shell (Fig. S3a). After a prolonged reaction for 45 h, the thickness of immobilized  $\gamma$ -AlOOH nanosheets increased (Fig. S3b) and the void space between the core and shell became larger. Part of the  $\text{SiO}_2$  shell was dissolved and a non-continuous shell was observed. By further increasing the reaction time, the  $\text{SiO}_2$  shell totally disappeared and all the  $\gamma$ -AlOOH nanosheets were directly immobilized onto the  $\text{Fe}_3\text{O}_4$  core (Fig. S3c). Noticeably, almost no separated  $\gamma$ -AlOOH nanosheets were found (Fig. S3d–f) in the final  $\text{Fe}_3\text{O}_4@/\gamma$ -AlOOH product, thus tight connections between  $\gamma$ -AlOOH nanosheets existed (inset of Fig. S3e). Furthermore, when  $\text{Al}^{3+}$  was substituted by another metal ion, such as  $\text{Ni}^{2+}$ , interestingly, yolk-like  $\text{Fe}_3\text{O}_4@/\text{NiSiO}_3$  core/shell spheres were obtained (Fig. S2d). As a result, the flower-like structures with desirable composition could be only produced under optimized conditions by utilizing the interplay and synergy of alkaline etching and hydrolysis reaction.

Au nanoparticles (4 nm) can be further self-assembled (Fig. 3a–c) onto the surfaces of the hierarchical  $\gamma$ -AlOOH

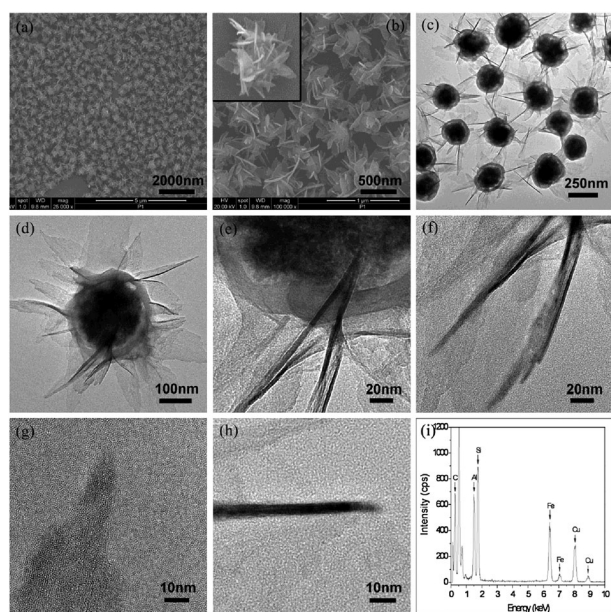


**Fig. 2** SEM images (a and b), TEM images (c–h), and EDX spectrum (i) of the  $\text{Fe}_3\text{O}_4@/\text{SiO}_2@/\gamma$ -AlOOH flower-like structures.

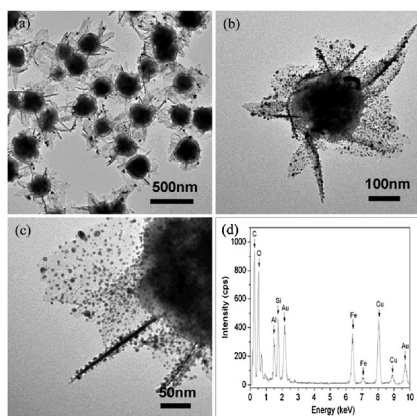


**Fig. 3** TEM images (a–c), and EDX spectrum (d) of the  $\text{Fe}_3\text{O}_4@SiO_2@ \gamma\text{-AlOOH}@Au$  flower-like structures.

nanosheets to form  $\text{Fe}_3\text{O}_4@SiO_2@ \gamma\text{-AlOOH}@Au$  flowers via an electrostatic attraction without forming large aggregates.<sup>9</sup> The EDX spectrum (Fig. 3d) reveals that the particle contains four elements—Fe, Si, Al, and Au, which agreed well with the XRD result (Fig. S1c). Furthermore, the localized Au nanoparticles could act as nucleation centers for Au, enhancing the overall loading percentage of Au of the microflowers. The weight % of Au could be controlled by a number of repeated  $\text{HAuCl}_4$  reductions with ascorbic acid (Fig. S4). The growth cycles of Au nanoparticles on the  $\gamma\text{-AlOOH}$  surfaces possess substantial changes in their absorption spectra (Fig. S5), at 420 and 520 nm.<sup>12</sup>

Hierarchical nanostructures possess large surface area and void space endowed by the unique structures, thus leading to enhanced performance.<sup>13</sup> The  $\text{Fe}_3\text{O}_4@SiO_2@ \gamma\text{-AlOOH}@Au$  nanoflowers can be applied as adsorbents to remove proteins from solution or in contrast, to immobilize proteins for specific functions.<sup>14</sup> Bovine serum albumin (BSA, > 66 kDa), a most abundant protein in bovine blood, was chosen as a typical protein for study. Starting with an initial  $0.1 \text{ mg mL}^{-1}$  of BSA solution, 25% ( $19.3 \text{ mg g}^{-1}$ ) of BSA was removed at room temperature, monitoring at 280 nm of the absorption spectra (Fig. 4). Furthermore, with increasing BSA concentration, the removal/immobilization capacity of the nanoflowers increases and reaches  $369.3 \text{ mg g}^{-1}$  (inset of Fig. 4). The high surface area in the void nano-space of the nanosheets and the charge

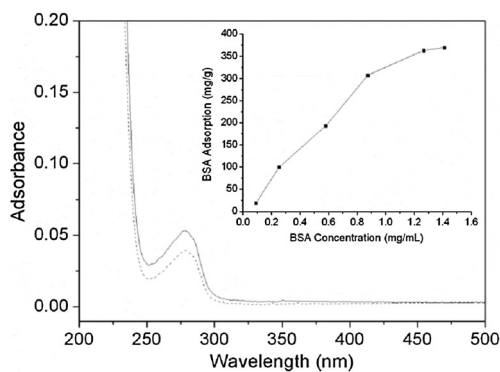


**Fig. 4** UV/visible absorption spectra of the BSA solution before (solid) and after (dash) adsorption. Inset: the immobilization/removal capacity of BSA at different concentrations.

compatibility between Au nanoparticles/ $\gamma\text{-AlOOH}$  and BSA presumably facilitated a favorable multivalent binding. The  $\text{Fe}_3\text{O}_4@SiO_2@ \gamma\text{-AlOOH}@Au$  nanoflowers are indeed superparamagnetic which is inherited from the magnetic  $\text{Fe}_3\text{O}_4$  core particles.<sup>6b</sup> This will provide an efficient way to separate these particles from a sol or a suspension system (Fig. S8) under an externally applied magnetic field.

In conclusion, magnetic responsive  $\text{Fe}_3\text{O}_4@SiO_2@ \gamma\text{-AlOOH}@Au$  nano/micro-flowers were synthesized. By way of an example, these magnetic micro/nano-structures were employed to immobilize/remove BSA protein. Eventually, this material could be applicable in enzyme immobilization for specific catalytic functions, drug/gene delivery, and selective capture of biomolecules for water purification, in addition to their efficient magnetic separation and targeting properties.

We acknowledge the financial support by RGC-GRF (CUHK401709) and UGC (AoE/P-03/08) research grants.

## Notes and references

- (a) S. H. Yu, M. Antonietti, H. Colfen and J. Hartmann, *Nano Lett.*, 2003, **3**, 379; (b) Y. Q. Wang, G. Z. Wang, H. Q. Wang, C. H. Liang, W. P. Cai and L. D. Zhang, *Chem.–Eur. J.*, 2010, **16**, 3497; (c) C. Z. Wu, Y. Xie, L. Y. Lei, S. Q. Hu and C. Z. Ouyang, *Adv. Mater.*, 2006, **18**, 1727; (d) C. Chen, W. Chen, J. Lu, D. R. Chu, Z. Y. Huo, Q. Peng and Y. D. Li, *Angew. Chem., Int. Ed.*, 2009, **48**, 4816.
- (a) P. D. Yang, T. Deng, D. Y. Zhao, P. Y. Feng, D. Pine, B. F. Chmelka, G. M. Whitesides and G. D. Stucky, *Science*, 1998, **282**, 2244; (b) L. S. Zhong, J. S. Hu, H. P. Liang, A. M. Cao, W. G. Song and L. J. Wan, *Adv. Mater.*, 2006, **18**, 2426; (c) Y. Huang, H. Q. Cai, D. Feng, D. Gu, Y. H. Deng, B. Tu, H. T. Wang, P. A. Webley and D. Y. Zhao, *Chem. Commun.*, 2008, 2641.
- Y. H. Deng, Y. Cai, Z. K. Sun, J. Liu, C. Liu, J. Wei, W. Li, C. Liu, Y. Wang and D. Y. Zhao, *J. Am. Chem. Soc.*, 2010, **132**, 8466.
- (a) S. L. Xiong, B. J. Xi, C. M. Wang, G. F. Zou, L. F. Fei, W. Z. Wang and Y. T. Qian, *Chem.–Eur. J.*, 2007, **13**, 3076; (b) Y. Q. Wang, G. Z. Wang, H. Q. Wang, W. P. Cai, C. H. Liang and L. D. Zhang, *Nanotechnology*, 2009, **20**, 155604; (c) C. Bae, Y. J. Yoon, W. S. Yoon, J. Moon, J. Y. Kim and H. J. Shin, *ACS Appl. Mater. Interfaces*, 2010, **2**, 1581.
- (a) W. S. Choi, H. Y. Koo and D. Y. Kim, *Adv. Mater.*, 2007, **19**, 451; (b) Q. Zhang, T. R. Zhang, J. P. Ge and Y. D. Yin, *Nano Lett.*, 2008, **8**, 2867.
- (a) J. P. Ge and Y. D. Yin, *Adv. Mater.*, 2008, **20**, 3485; (b) S. H. Xuan, Y. X. J. Wang, J. C. Yu and K. C.-F. Leung, *Chem. Mater.*, 2009, **21**, 5079.
- S. Laurent, D. Forge, M. Port, A. Roch, C. Robic, L. V. Elst and R. N. Muller, *Chem. Rev.*, 2008, **108**, 2064.
- (a) J. Kim, Y. Z. Piao, N. Lee, Y. I. Park, I. H. Lee, J. H. Lee, S. R. Paik and T. Hyeon, *Adv. Mater.*, 2010, **22**, 57; (b) H. M. Chen, X. H. Lu, C. H. Deng and X. M. Yan, *J. Phys. Chem. C*, 2009, **113**, 21068.
- (a) C. L. Fang, K. Qian, J. Zhu, S. Wang, X. Lv and S. H. Yu, *Nanotechnology*, 2008, **19**, 125601; (b) S. H. Xuan, Y. X. J. Wang, J. C. Yu and K. C.-F. Leung, *Langmuir*, 2009, **25**, 11835.
- H. Q. Cao, L. Zhang, X. W. Liu, S. C. Zhang, Y. Liang and X. R. Zhang, *Appl. Phys. Lett.*, 2007, **90**, 193105.
- (a) J. B. Fei, Y. Cui, X. H. Yan, W. Qi, Y. Yang, K. W. Wang, Q. He and J. B. Li, *Adv. Mater.*, 2008, **20**, 452; (b) P. M. Arnal, C. Weidenthaler and F. Schuth, *Chem. Mater.*, 2006, **18**, 2733.
- Q. Zhang, J. P. Ge, J. Goebel, Y. X. Hu, Y. G. Sun and Y. D. Yin, *Adv. Mater.*, 2010, **22**, 1905.
- X. W. Lou, C. Yuan and L. A. Archer, *Adv. Mater.*, 2007, **19**, 3328.
- (a) Y. H. Deng, D. W. Qi, C. H. Deng, X. M. Zhang and D. Y. Zhao, *J. Am. Chem. Soc.*, 2008, **130**, 28; (b) K. C.-F. Leung, H. P. Ho, Y. W. Kwan and S. K. Kong, *Expert Rev. Mol. Diagn.*, 2010, **10**, 863.